The Journal of Experimental Biology 216, 2293-2301

doi:10.1242/jeb.082479

RESEARCH ARTICLE

Hypoxia-induced compression in the tracheal system of the tobacco hornworm caterpillar, *Manduca sexta*

Kendra J. Greenlee[1,*], John J. Socha[2], Haleigh B. Eubanks[3], Paul Pedersen[1], Wah-Keat Lee[4] and Scott D. Kirkton[5]

[1]Department of Biological Sciences, North Dakota State University, Fargo, ND 58108, USA, [2]Department of Engineering Science and Mechanics, Virginia Tech, Blacksburg, VA 24061, USA, [3]Department of Biology, Jackson State University, Jackson, MS 39217, USA, [4]X-Ray Science Division, Advanced Photon Source, Argonne National Laboratory, Argonne, IL 60439, USA and [5]Department of Biological Sciences, Union College, Schenectady, NY 12308, USA

*Author for correspondence (kendra.greenlee@ndsu.edu)

SUMMARY

Abdominal pumping in caterpillars has only been documented during molting. Using synchrotron X-ray imaging in conjunction with high-speed flow-through respirometry, we show that *Manduca sexta* caterpillars cyclically contract their bodies in response to hypoxia, resulting in significant compressions of the tracheal system. Compression of tracheae induced by abdominal pumping drives external gas exchange, as evidenced by the high correlation between CO_2 emission peaks and body movements. During abdominal pumping, both the compression frequency and fractional change in diameter of tracheae increased with body mass. However, abdominal pumping and tracheal compression were only observed in larger, older caterpillars (>0.2 g body mass), suggesting that this hypoxic response increases during ontogeny. The diameters of major tracheae in the thorax increased isometrically with body mass. However, tracheae in the head did not scale with mass, suggesting that there is a large safety margin for oxygen delivery in the head in the youngest animals. Together, these results highlight the need for more studies of tracheal system scaling and suggest that patterns of tracheal investment vary regionally in the body.

Supplementary material available online at http://jeb.biologists.org/cgi/content/full/216/12/2293/DC1

Key words: insect, respiration, tracheae, ventilation, caterpillar.

Received 1 November 2012; Accepted 6 March 2013

INTRODUCTION

Insects breathe using a tracheal respiratory system. The tracheal system consists of a series of branching tubes that decrease in size from their origin at the spiracles, which are valved openings to the atmosphere. In some species, muscular contractions coordinated with opening and closing of the spiracular valves convectively deliver oxygen to the tissues. The tracheal respiratory system is efficient, allowing insects to tolerate very low oxygen levels [<2 kPa partial pressure of O_2 (P_{O_2}) (Harrison et al., 2006)]. Insects from several orders are known to use abdominal pumping to unidirectionally drive air flow through the tracheal system (Harrison, 2009). During hypoxia, abdominal pumping often increases as a compensatory response to increase airflow to tissues (Greenlee and Harrison, 2004a). Older, larger *Schistocerca americana* grasshoppers rely more on abdominal pumping at low P_{O_2} levels, suggesting that this behavior is an important response to hypoxia (Greenlee and Harrison, 2004a).

Insects that lack obvious mechanisms for producing major convective airflows would not be expected to be as tolerant of hypoxia. Caterpillars typically do not exhibit abdominal pumping behavior, and although a few mechanisms of producing convective airflows have been proposed [e.g. hemolymph pressure changes (Wasserthal, 1996) and passive suction ventilation (Kestler, 1985)], the relative role of convection *versus* diffusion in the tracheal system of caterpillars is not well understood. Despite the lack of obvious external ventilatory mechanisms, *Manduca sexta* L. caterpillars of all ages are surprisingly tolerant of hypoxia. For example, the average oxygen level below which *M. sexta* metabolism can no longer be sustained, the critical P_{O_2}, was shown to be 5 kPa (Greenlee and Harrison, 2005), comparable to that of species with known mechanisms of convective ventilation. In addition, the largest larvae have been observed to feed in P_{O_2} levels as low as 1 kPa (Greenlee and Harrison, 2005), suggesting that size-related compensatory mechanisms for gas exchange may exist. During the course of this previous study, we observed that, when exposed to hypoxia, the older, larger caterpillars exhibited movements resembling abdominal pumping. Although this behavior had not been previously documented in non-molting caterpillars, we suspected that the body movements were a respiratory-related response, perhaps functioning to increase convective gas exchange during hypoxic exposure.

Here, we test the hypothesis that the external body movements play a role in gas exchange in *M. sexta* larvae by stimulating abdominal pumping with hypoxia (<3 kPa P_{O_2}). We used high-speed flow-through respirometry alone and with X-ray imaging to visualize the tracheal system during abdominal pumping. In the first set of trials without X-ray imaging, high-speed flow-through respirometry enabled the resolution of individual expirations of CO_2, which could be correlated with body movements in hypoxia. In other trials, we combined respirometry, X-ray imaging and light video imaging to determine whether the external body movements observed in hypoxia resulted in internal changes in the tracheal system. Because

the abdominal pumping movements were only observed in the largest caterpillars, we also tested the hypothesis that the oxygen delivery capacity of larger caterpillars does not match the increase in oxygen demand with increasing body mass.

MATERIALS AND METHODS

Animals

Manduca sexta larvae were reared from eggs (Carolina Biological Supply, Burlington, NC, USA) with *ad libitum* access to a wheat-germ-based artificial diet (Ojeda-Avila et al., 2003). Animals were reared at 25°C on 16 h:8 h light:dark cycles and weighed prior to experiments. Caterpillars ranged in age from first to fifth instar (mass range: 0.001–6.95 g) and were within the first half of each instar based on their molting dates, body masses and head widths.

Respirometry

We used CO_2 emission as an index of oxygen consumption. High-speed, flow-through respirometry was used to measure CO_2 emission of caterpillars at room temperature (24±1°C) with and without the use of synchrotron X-ray imaging at Argonne National Laboratory and North Dakota State University (NDSU), respectively. Trials without X-ray imaging (N=7 caterpillars) used chambers constructed of 60 ml syringes that had been plumbed with flexible tubing. Chamber volume was adjusted based on the animal's body size. Animals were placed in chambers and allowed to acclimate for 20 min. Dry, CO_2-free air (Balston purge gas generator, Parker, Cleveland, OH, USA) was pushed through the chamber at various flow rates (50–5000 ml min^{-1}) based on animal size, using a mass flow controller (MFC-4, Sable Systems, Las Vegas, NV, USA) and mass flow meters (Sierra Instruments, Monterey, CA, USA). The time constant averaged 28±3.3 s. Hypoxic gas mixes (0, 1, 2, 3 or 5 kPa P_{O2}) were generated by diluting the air stream with N_2. Water was removed from excurrent air using $MgClO_4$ and the fraction of CO_2 was measured using a Li-Cor 7000 infrared gas analyzer (Li-Cor Biosciences, Lincoln, NE, USA). During experiments with X-ray imaging (N=37 caterpillars), the respirometry system was the same, except that chambers were constructed of optically clear acrylic and X-ray transparent polyimide film (Kapton, DuPont, Wilmington, DE, USA), as previously described (Greenlee et al., 2009). In addition, incurrent gas mixes were generated from O_2 and N_2 tanks and scrubbed of water and CO_2 using a drierite/ascarite/drierite column. CO_2 emission rates were recorded in normoxia pre- and post-beam exposure. All caterpillars were exposed to decreasing levels of atmospheric oxygen followed by a recovery period in normoxia. In experiments without X-ray imaging, animals were exposed to P_{O2} levels of 21, 5, 3 and 0 kPa. Experiments with X-ray exposure used P_{O2} levels of 21, 2, 1 and 0 kPa.

Synchrotron X-ray imaging

Caterpillars were shipped overnight from NDSU to the Advanced Photon Source (Argonne National Laboratory, Argonne, IL, USA) and were given *ad libitum* access to food. Tracheae in live caterpillars were visualized using synchrotron X-ray phase-contrast imaging with a 2× or 5× objective lens and a Cohu-cooled, charge-coupled device video camera as previously described (Socha et al., 2007). Resulting fields of view for each lens were 2.4×1.8 mm and 0.96×0.72 mm, respectively, with corresponding resolutions of approximately 5 and 2 μm. The distance from the sample to the scintillator (which converted X-rays to visible light) ranged from 0.8 to 1 m, and the monochromatic X-ray energy was 25 kev. Video was recorded to mini-DV tapes using a camcorder (TRV-900, Sony, Tokyo, Japan). A metal grid (400 lines per inch) was placed in the beam as a scale for spatial calibration of the X-ray images. Caterpillars were placed in respirometry chambers on a remote-controlled stage that allowed us to move the insect within the beam and to focus on specific body regions, as previously described (Greenlee et al., 2009). Exposure to X-ray radiation in a typical experiment was no longer than 15 min.

To determine whether and how tracheal structure and function changed during breathing in hypoxia, we used the X-ray videos to measure changes in tracheal diameter and compression frequency. X-ray videos were first digitized and converted to image sequences using ImageJ software (National Institutes of Health, Bethesda, MD, USA). Image sequences were viewed and tracheal compression cycles were identified. Each cycle had an observed maximum and minimum tracheal diameter. Three compression cycles from each P_{O2} from the abdomen of each caterpillar were analyzed for tracheal diameter (N=43 caterpillars). When tracheae compressed, the frames with the largest and the smallest diameters were selected for measurement. Tracheal diameters were measured using ImageJ, with a measurement uncertainty of 1.2%. For sequences without any compression cycles, we digitized 20 consecutive video frames, with the starting point of the cycle selected arbitrarily. We calculated the fraction of compression by taking the change in diameter as a percent of the maximum diameter and averaging this for the three breaths from each P_{O2}. Fractional data were arc-sine transformed for statistical analysis. We also counted the number of tracheal compressions in 30 s to calculate compressions per minute (N=22 caterpillars).

Measurement of tracheal diameter

To investigate the scaling of tracheal structures with body size in larval *M. sexta*, we used synchrotron X-ray imaging to create high-resolution projection images of the tracheal system of euthanized animals. Caterpillars within the first half of each instar of a range of sizes (0.0019 to 1.591 g) were euthanized with ethyl acetate, chilled to stabilize residual internal motion, and warmed to room temperature before X-ray imaging. Animals were placed upright in polyimide tubing on the movable stage. Because the field of view was smaller than the animal, multiple images were required to image entire caterpillars. For each specimen, composite images were created first by linearly translating the sample and capturing X-ray images that successively overlapped by ~30%, and then stitching them together using a custom MATLAB program (MathWorks, Natick, MA, USA). Images were captured using a CCD camera (Sensicam, Cooke Corporation, Romulus, MI, USA), which provided higher spatial resolutions than those achievable with the live video system. We directly measured the width of major tracheae in X-ray images (N=16 caterpillars) using ImageJ. Specific tracheae were recognized using morphological characters identified by Eaton (Eaton, 1988).

Statistics

Means ± s.e.m. are presented throughout. Statistical analyses were performed using SPSS version 19 (IBM, Armonk, NY, USA) and SigmaPlot version 11 (Systat Software, San Jose, CA, USA). P-values <0.05 were considered to be statistically significant.

To test the effect of P_{O2} on the ratio of CO_2 peaks to abdominal pumps, repeated-measures ANOVA (RM-ANOVA) was used. Because each animal was exposed to multiple P_{O2} levels, P_{O2} was the within-subjects factor and mass was a covariate.

To test for differences in CO_2 emission rates, log-transformed data were subjected to RM-ANOVA with treatment as the within-

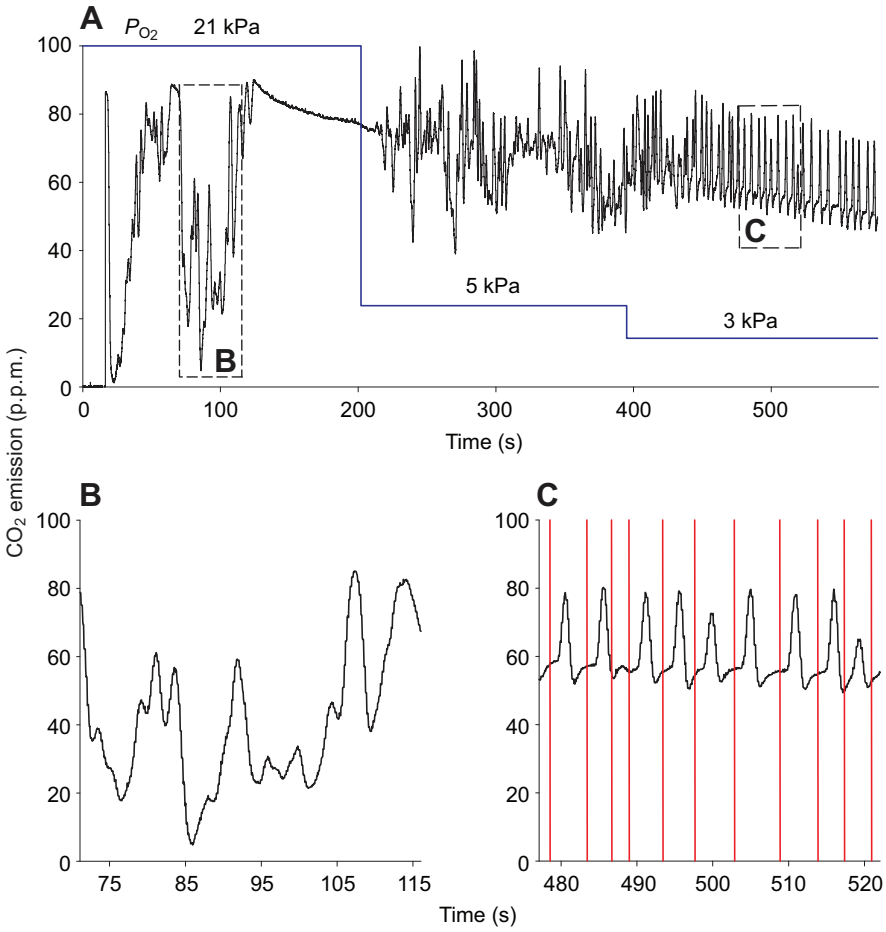

Fig. 1. (A) Representative patterns of CO_2 emission from one fifth instar *Manduca sexta* over the entire trial. Boxes indicate expanded sections of (B) normoxic breathing during which no external body movements were observed and (C) during hypoxic exposure (3 kPa P_{O_2}), when external pumping was observed. Red lines in C indicate the timing of observed body contractions. No contractions were observed in normoxia.

subjects factor (levels include pre-beam normoxia, normoxia with X-ray, 2 kPa P_{O_2}, 1 kPa P_{O_2}, anoxia and recovery in normoxia) and body mass as a covariate. We then calculated the linear regression between CO_2 emission and body mass for each within-subjects factor and compared 95% confidence intervals (CI) of slopes.

To assess the relationships between the fractional change in tracheal diameter and tracheal compression frequency with body mass, we used two approaches. First, data were log transformed and analyzed using RM-ANOVA with P_{O_2} as the within-subjects repeated factor and log-transformed body mass as the covariate. Second, because only large animals exhibited abdominal pumping, we binned the data. We classified animals by size, as either large (>0.2 g) or small (<0.2 g) and used RM-ANOVA with P_{O_2} as the within-subjects factor, size as the between-subjects factor and mass as the covariate.

To determine the relationship between tracheal diameter and body mass, data were log transformed and subjected to linear regressions of each trachea on body mass. Because there may be correlations between tracheae, we also grouped tracheae according to body segment and used a multivariate general linear model with log-transformed body mass as a covariate. Tracheae from the head and thorax were in one group, while abdominal tracheae from the first four segments were grouped. In addition, because each caterpillar had multiple tracheal measurements, we used RM-ANOVA with trachea as the within-subjects factor and mass as a covariate. We used three methods to determine whether the multiple comparisons were significant. First, we corrected the *P*-values for 15 multiple comparisons using the Bonferroni correction ($1–\alpha/k$, where α=0.05 and k is the number of comparisons), decreasing the significance level to 0.003. Because the Bonferroni correction for multiple comparisons is very conservative and known to reduce power (Benjamini and Hochberg, 1995; Narum, 2006), we used two other methods. As our data are dependent and have a large number of comparisons, we used the false discovery rate (FDR) method, which

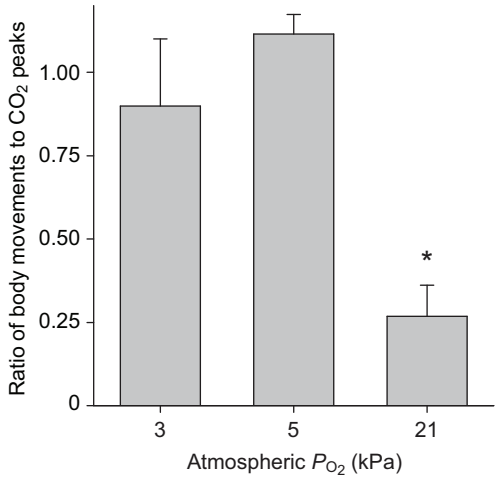

Fig. 2. In hypoxia (3 or 5 kPa P_{O_2}), CO_2 emission peaks were significantly more correlated with external caterpillar body movements than in normoxia (21 kPa P_{O_2}) (*P<0.05).

results in an adjusted significance level of 0.033, and a modified FDR method, which results in a significance level of 0.015 (Benjamini and Hochberg, 1995; Benjamini and Yekutieli, 2001; Narum, 2006).

RESULTS

In normoxia, the pattern of CO_2 emission of caterpillars was continuous and irregular (Fig. 1A,B, supplementary material Movie 1). In addition, external body movements were not correlated with CO_2 peaks (mean ratio=0.27±0.1; Fig. 2). As atmospheric P_{O_2} decreased, caterpillar abdomens began rhythmically contracting, and two types of pumping movements were observed. One resembled traditional abdominal pumping, where the abdominal segments shorten dorso-ventrally in concert along the entire length of the abdomen (supplementary material Movie 1). The other type of pumping resulted in dorso-ventral compression of each abdominal segment in series from the thorax to the posterior of the caterpillar. For the second type of pumping, we counted one series of contractions as one movement. Correlation of external body movements and CO_2 emission increased as atmospheric P_{O_2} decreased (RM-ANOVA, $F_{2,18}$=12.06, P<0.001; Fig. 1A,C, Fig. 2, supplementary material Movie 1). Responses to exposures of either 5 or 3 kPa P_{O_2} did not differ, and caterpillar CO_2 emission became cyclic and was nearly perfectly correlated with external body movement (mean ratio of CO_2 peaks to external body movements=1.01±0.11; Fig. 2).

To determine whether the external body movements we observed were driving compressive deformations of the tracheal system, we used the same method while recording X-ray video of caterpillars breathing in normoxia and hypoxia. CO_2 emission rates varied with treatment (RM-ANOVA, $F_{1,21}$=7.51, P<0.02; Fig. 3) and body mass (RM-ANOVA, $F_{1,21}$=24.94, P<0.01). Bonferroni-corrected

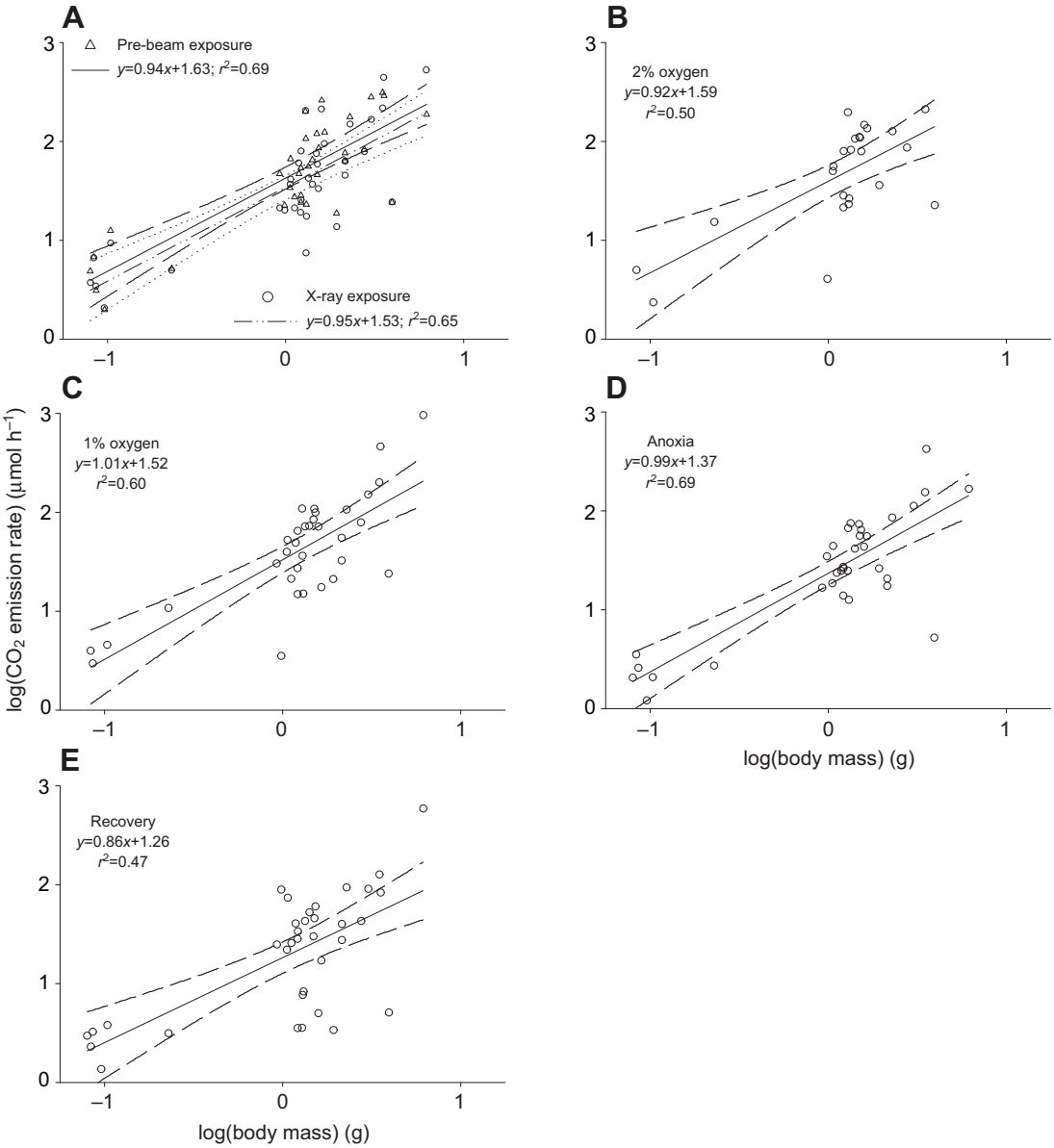

Fig. 3. CO_2 emission rates in *M. sexta*. (A) Normoxic CO_2 emission before (triangles) and during (circles) X-ray exposure were nearly identical, as evidenced by overlapping 95% CI (dashed and dotted lines). (B–E) Log–log plots of CO_2 emission rate *versus* body mass showed significant linear correlations at all P_{O_2} levels. Dashed lines show 95% CI.

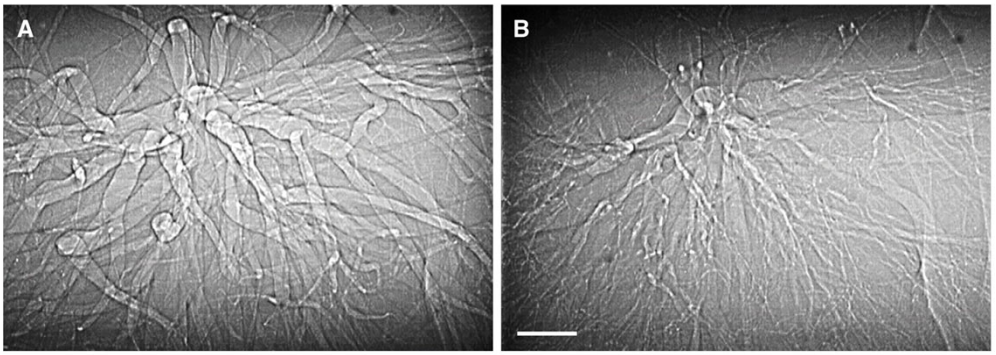

Fig. 4. X-ray images of a fifth instar *M. sexta* tracheal compression cycle. (A) Maximum and (B) minimum diameter of tracheae during exposure to 1 kPa P_{O_2}. Body mass, 2.78 g. Scale bar for both images, 250 µm.

post hoc tests showed that CO_2 emission rate only varied due to the effects of hypoxia; there was no effect of X-ray exposure on CO_2 emission rate. Regression lines of CO_2 emission *versus* log mass were not significantly different between pre-beam normoxic CO_2 emission and normoxic X-ray exposure (95% CIs for slope: pre-beam normoxia 0.39–1.19, X-ray normoxia 0.30–1.16; for *y*-intercept: pre-beam normoxia 1.49–1.81, X-ray normoxia 1.35–1.69; Fig. 3A). CO_2 emission rate varied with P_{O_2} treatment (RM-ANOVA, $F_{1,30}$=2.76, P<0.001) and with mass (RM-ANOVA, $F_{1,30}$=58.76, P<0.001). Mass scaling of CO_2 emission rate did not vary with P_{O_2}, as evidenced by overlapping 95% CI of slopes: 2 kPa PO_2, 95% CI=0.52–1.33; 1 kPa P_{O_2}, 95% CI=0.71–1.31; anoxia, 95% CI=0.76–1.24; recovery, 95% CI=0.54–1.18; Fig. 3).

In normoxia, the X-ray video showed that tracheae translated with external body movements, but tracheal diameters did not change (supplementary material Movie 2). During hypoxia exposure, the external body movements of large caterpillars were also highly correlated with CO_2 emission peaks. Furthermore, the external body movements during hypoxia co-occurred with the compression of many tracheal tubes (Fig. 4, supplementary material Movie 1). Fractional change in tracheal diameter in hypoxia, but not normoxia or anoxia, was significantly correlated with body mass (Fig. 5) at 1 and 2 kPa P_{O_2} (RM-ANOVA, P_{O_2} × mass interaction: $F_{2,80}$=3.57, P<0.04). Regressing fractional change of tracheal diameter in both 1 and 2 kPa P_{O_2} on body mass revealed significant logarithmic relationships [1 kPa: y=0.36(mass)$^{0.46}$, $F_{1,47}$=54.4, P<0.001; 2 kPa: y=0.29(mass)$^{0.39}$, $F_{1,40}$=22.31, P<0.001; Fig. 5]. However, because smaller caterpillars (mass <0.2 g) did not exhibit external body movements or tracheal compressions, we decided to bin the data into two groups and determine the effects of mass within each group. There was a significant interaction between P_{O_2} and size, indicating that smaller caterpillars responded differently to hypoxia than larger ones (RM-ANOVA, $F_{2,76}$=3.27, P<0.05). Within each size class (i.e. small or large) there was no effect of body mass (P=0.18), suggesting that there is a size threshold for tracheal compression (Fig. 5).

Compression frequency showed a pattern similar to that of compression fraction (Fig. 6). Compression frequency in hypoxia varied differently with P_{O_2} level, depending on the mass of the animal (RM-ANOVA, P_{O_2} × mass interaction: $F_{2,22}$=4.36, P<0.03; Fig. 6). The smallest animals had the lowest compression frequencies regardless of P_{O_2} treatment. There were no compressions at 21 kPa P_{O_2} and few in anoxia. However, at 1 and 2 kPa P_{O_2} there was a significant power relationship between compression frequency and body mass (2 kPa: $F_{1,13}$=10.69, P<0.01; 1 kPa: $F_{1,21}$=14.87, P<0.01; Fig. 6). Because the smallest caterpillars did not exhibit this behavior,

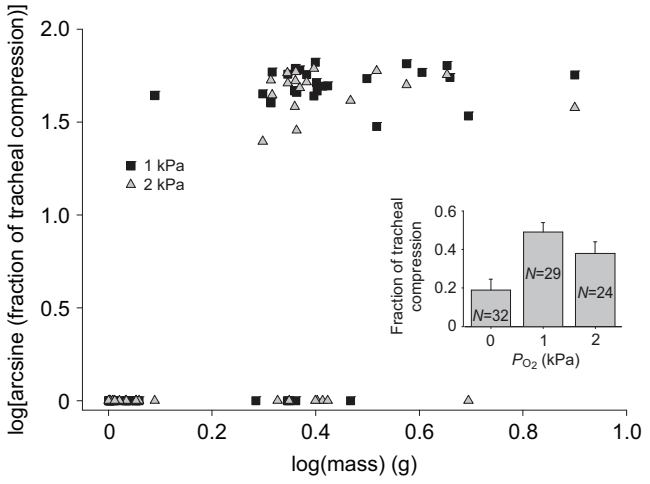

Fig. 5. Tracheal compression in *M. sexta* increased as P_{O_2} decreased and scaled positively with body mass. Fractional change in tracheal diameter per breath in 2 kPa P_{O_2} (gray triangles) and 1 kPa P_{O_2} (black squares) as a function of body mass. No compressions were exhibited in normoxia; therefore, those data are not shown. Inset: average fractional change in tracheal diameter for animals above 0.2 g as a function of P_{O_2}.

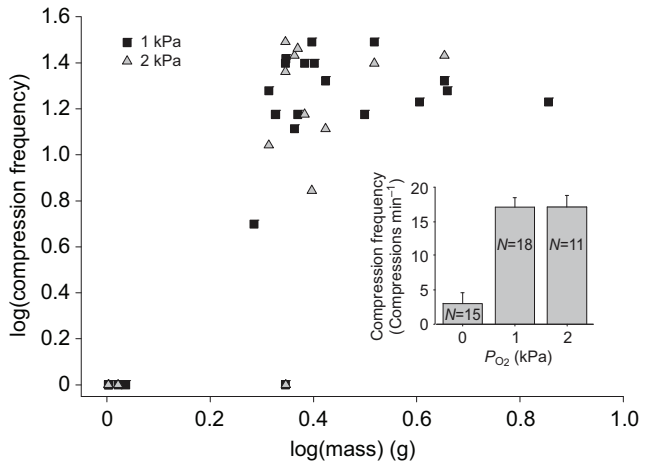

Fig. 6. *Manduca sexta* increased gas exchange by compressing their tracheae in hypoxia, but not in normoxia or anoxia. Compression frequency (compressions min^{-1}) as a function of body mass (g) at 1 kPa P_{O_2} (black squares) or 2 kPa P_{O_2} (gray triangles). No compressions were exhibited in normoxia; therefore, those data are not shown. Inset: average compression frequency for animals above 0.2 g as a function of P_{O_2}.

Table 1. Model parameters resulting from the linear regression of log-transformed tracheal diameter (μm) and body mass (g)

Body segment	Trachea location	*F*	d.f.	*P* (multivariate analysis)	*P* (repeated-measures analysis)	r^2	*b*	95% CI Lower bound	95% CI Upper bound	*y*	95% CI Lower bound	95% CI Upper bound
Head	HDT1	1.92	1,6	0.24	0.44	0.32	0.13	–0.13	0.38	1.59	1.19	1.99
	HDT2	0.82	1,6	0.42	0.73	0.17	0.09	–0.19	0.37	1.50	1.06	1.94
	HDT3	2.62	1,6	0.18	0.34	0.40	0.13	–0.09	0.36	1.58	1.22	1.93
Thorax	mesoMT	14.12	1,6	0.02[a]	0.06	0.78	0.22	0.06	0.38	1.45	1.19	1.70
	mesoTT	7.09	1,6	0.06	0.13	0.64	0.21	–0.01	0.43	1.61	1.27	1.96
	mesoVTT	26.82	1,6	0.01[a,b]	0.03[b]	0.87	0.27	0.13	0.42	1.34	1.11	1.57
	metaTT	9.84	1,6	0.03[b]	0.08	0.71	0.25	0.03	0.48	1.44	1.13	1.74
	metaDT	21.28	1,6	0.01[a,b]	0.03[b]	0.84	0.32	0.13	0.51	1.60	1.24	1.95
Abdomen	1DT	4.44	1,10	0.07	0.02[b]	0.36	0.15	–0.02	0.32	1.10	0.84	1.36
	1TT	3.75	1,10	0.09	0.06	0.32	0.11	–0.02	0.25	1.52	1.31	1.72
	2DT	2.00	1,10	0.19	0.04	0.20	0.13	–0.08	0.34	1.02	0.70	1.34
	3DT	2.65	1,10	0.14	0.05	0.25	0.12	–0.05	0.29	1.01	0.74	1.27
	3TT	1.91	1,10	0.20	0.03[b]	0.19	0.10	–0.07	0.27	1.45	1.18	1.71
	4DT	0.25	1,10	0.63	0.13	0.03	0.04	–0.15	0.24	1.03	0.73	1.33
	4VTT	3.51	1,10	0.10	0.02[b]	0.31	0.08	–0.02	0.18	1.25	1.10	1.40

Equations are in the form of log(tracheal diameter) = [*b* × log(body mass)] + *y*.
See Fig. 7 for tracheae locations. hd, head; meso, mesothorax; meta, metathorax; DT, dorsal trachea; TT, transverse tracheae; VTT, ventral transverse trachea. Numbers preceding trachea name indicate the abdominal segment in which the trachea was measured.
Sample size = 16 caterpillars ranging in mass from 0.0019 to 1.591 g.
[a]Significant when using false discovery rate (FDR)-adjusted significance level of 0.033.
[b]Significant when using modified FDR-adjusted significance level of 0.015.

we again analyzed the grouped data. There was a significant effect of size on compression frequency, with larger animals having higher frequency than smaller animals ($F_{1,16}$=6.28, P<0.03). Within each group, there was no effect of body mass (P=0.996), suggesting that there is a threshold for tracheal compression (Fig. 6).

To determine how tracheal structure varied with body size, we measured the diameter of major tracheae throughout the head, thorax and abdomen of caterpillars of a range of sizes (N=16). We analyzed these data in two ways. First, tracheae were divided into two groups for multivariate analysis: head and thoracic tracheae were grouped, and abdominal segments 1–4 were grouped. Tracheae from abdominal segments 5–10 were excluded, as the most posterior abdominal segments from the largest animals could not be visualized with our imaging setup. Four out of 15 tracheae measured showed statistically significant correlations with body mass (Table 1, Figs 7, 8). Slopes of log-transformed data ranged from 0.04 in the dorsal trachea of the fourth abdominal segment to 0.32 in the metathoracic dorsal trachea (Table 1). RM-ANOVA showed a significant interaction between trachea and body mass, indicating that not all tracheae were similarly correlated with mass ($F_{14,42}$=3.41, P<0.01). Parameter estimates from this analysis indicated significant correlations between body mass and several of the tracheae (Table 1). Bonferroni-corrected P-values showed that there was no relationship between tracheal diameter and mass. FDR and modified FDR-corrected P-values showed that some tracheae scaled positively with mass. Between both analyses, tracheae in the head consistently did not scale with body mass.

DISCUSSION

Here, we describe the first observations of abdominal pumping being used for gas exchange in the caterpillar *M. sexta*. These external body movements during hypoxia resulted in substantial tracheal compression, which appeared to be the driving force for gas exchange, as evidenced by the high correlation between CO_2 emission peaks and body movements (Figs 1, 2). Tracheal compression frequency and fractional change in tracheal diameter both increased as P_{O_2} level decreased. In addition, compression frequency and fractional change in diameter increased with body mass. Interestingly, smaller caterpillars did not employ abdominal pumping in response to hypoxia, nor did they exhibit tracheal compression. These size trends suggest that larger caterpillars require greater amounts of convection to satisfy gas exchange needs.

Metabolic rate, as indicated by the rate of CO_2 emission, scaled proportionally with body mass, across the range of masses used for metabolic measures (Fig. 3A). The scaling coefficients are consistent with previous work, showing that across instars, metabolic rates of *M. sexta* larvae scale with body mass$^{0.98}$ (Greenlee and Harrison, 2005) or with body mass$^{0.94}$ (Sears et al., 2012). Larval and pre-pupal silkworms, *Bombyx mori*, also have metabolic scaling coefficients near 1 [0.96–1.49 (Blossman-Myer and Burggren, 2010)]. Ontogenetic scaling relationships are typically more variable than the commonly described allometric scaling of mammalian metabolic rates (Glazier, 2005). One proposed explanation for higher scaling coefficients is that increased epidermal cell growth prior to molting requires increased oxygen consumption (Blossman-Myer and Burggren, 2010). Clearly, more work is needed to fully understand the underlying parameters that determine metabolic scaling in juvenile insects.

To our knowledge, this is the first description of abdominal pumping in lepidopteran larvae in response to low oxygen. We analyzed both the frequency of tracheal compression and the fractional change in tracheal diameter as a function of body size and P_{O_2}. The fractional change in tracheal diameter that occurred in hypoxia scaled logarithmically with body mass (scaling coefficient 0.46 or 0.39 depending on P_{O_2}; Fig. 5), with the largest number of caterpillars that compressed their tracheae occurring in 1 kPa P_{O_2}. Compression frequency also showed a statistically significant relationship with body mass, scaling with mass$^{0.31}$ or mass$^{0.5}$ depending on P_{O_2} (Fig. 6). In vertebrates, breathing frequency and tidal volume scale with mass$^{-0.25}$ and mass^{1}, respectively (Peters, 1983). Our comparable parameters, compression frequency and fractional change in tracheal diameter, did not scale with body mass in that way. An interspecific comparison of grasshoppers found mass

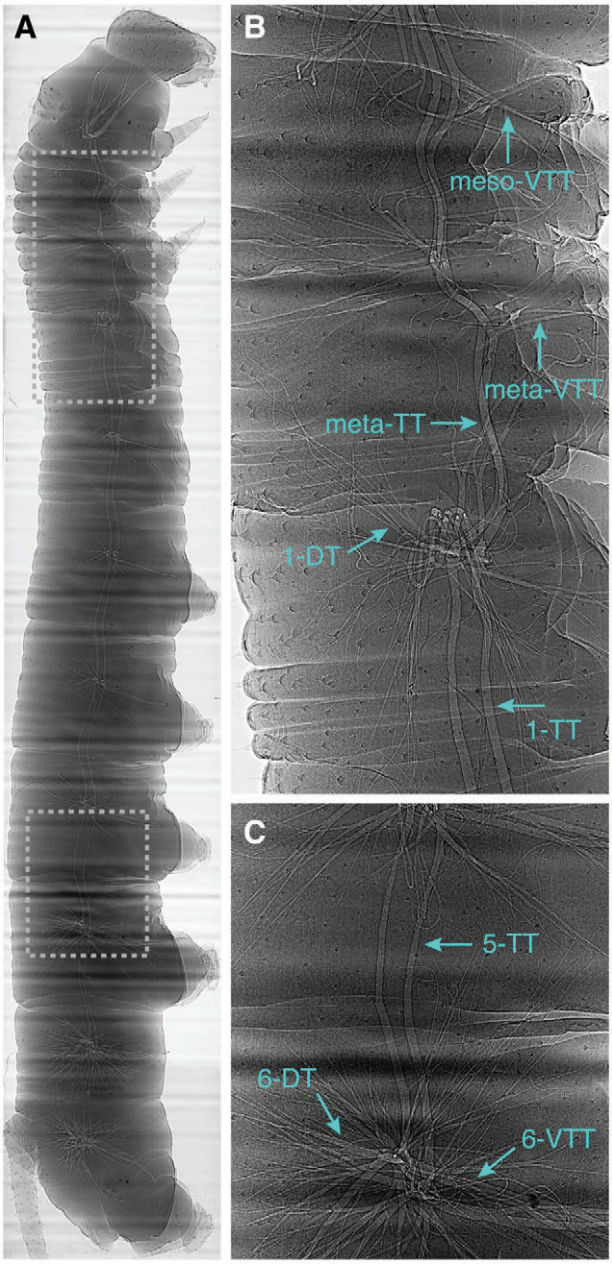

Fig. 7. (A) Composite X-ray image of a *M. sexta* larva (body mass 0.044 g). Boxes indicate enlarged views of tracheae in the anterior (B) and posterior (C) of the animal that showed a significant increase with body mass. VTT, ventral transverse trachea; DT, dorsal trachea; TT, transverse tracheae.

scaling relationships of ventilation frequency (0.23 in hypoxia) and tidal volume (0.71 in hypoxia) similar to our findings here (Greenlee et al., 2007).

Although we were able to fit statistically significant regressions to both parameters as a function of body mass, there was a distinct lack of response in the smallest caterpillars. Similar to our current findings, young grasshoppers also did not increase abdominal pumping in response to hypoxia. In *S. americana*, the critical P_{O_2} values for abdominal pumping were low across all instars and were lower than the critical P_{O_2} for CO_2 emission, indicating that the low oxygen does not limit muscle contraction (Greenlee and Harrison, 2004b). Indeed, young *M. sexta* larvae have critical P_{O_2} values for CO_2 emission similar to the largest, oldest caterpillars [5 kPa P_{O_2} (Greenlee and Harrison, 2005)], but here we observed abdominal pumping and tracheal compression only in the largest larvae (Figs 5, 6). Interestingly, these large specimens were still able to maintain abdominal pumping movements in atmospheres as low as 1 kPa P_{O_2} (Figs 5, 6). When we analyzed data from animals larger than 0.2 g that exhibited the pumping behavior, we found no significant mass scaling relationship with compression frequency or fractional change in diameter. One possibility is that the range of body masses analyzed needs to be increased. However, taken together with the findings in small grasshoppers, these data strongly suggest that there is a size threshold for this behavior. This may indicate that the largest caterpillars are unable to meet oxygen demands associated with their massive growth without abdominal pumping. To conclusively determine whether the lack of response to hypoxia in the youngest juveniles is a general developmental respiratory pattern for insects, many more species need to be tested.

Because we found that only large caterpillars exhibited abdominal pumping in hypoxia, we suspected that they had reduced oxygen delivery capacity. We analyzed tracheal investment using the diameter of individual tracheae. Based on geometric similarity, isometric scaling of a structure's diameter is predicted to scale with body mass$^{0.33}$ (Calder, 1981). Using multivariate analyses, four of the tracheae showed significant correlations with mass, and all of these exhibited scaling coefficients that were not different from 0.33, as evidenced by the overlap in the 95% CI. Using regressions generated by RM-ANOVA, many more tracheae scaled positively with body mass. Because many of the measured tracheae exhibited nearly significant correlations with mass, increasing the sample size may reveal significant scaling relationships (Table 1). Interestingly, the tracheae that exhibited significant mass scaling were all located in the thoracic and abdominal segments. Tracheae in the head did not scale with mass regardless of the type of analysis or multiple comparison adjustment, suggesting that tracheae in the head have a large safety margin for oxygen delivery in the younger, smaller animals (Fig. 8, Table 1). Alternatively, this would explain the increased use of convection observed in the older, larger animals. Whole-animal tracheal volume in *M. sexta*, measured by water displacement, scaled isometrically with body mass across the third, fourth and fifth instars (Callier and Nijhout, 2011), suggesting that differences in regional tracheal system investment may vary dramatically, which highlights the need for better measures of regional tracheal volumes. For example, our measures only account for changes in major tracheae, whereas measures using water displacement could include growth of smaller structures that would be more likely to increase and proliferate during development. In addition, the water displacement method may result in overfilling of tracheae and, thus, overestimation of tracheal volumes. In support of our current findings, however, another study using a similar X-ray technique to estimate sizes of tracheal system structures found that developing *S. americana* grasshoppers show differences in regional tracheal investment, with scaling coefficients for tracheae of 0.128 in the head and 0.067 in the thorax (Greenlee et al., 2009). Because there are trade-offs between tracheal investment and non-respiratory structures, one possible explanation for the lack of scaling relationships found in the head is that other tissues or organs, such as the gut, incur greater functional demands with increasing age, relative to the tracheal system. Alternatively, tracheae in the head may need to be proportionally smaller for some other functional reason, perhaps related to hemolymph volume demands or muscular constraints. This also fits with our finding that larger animals respond to low P_{O_2} levels by increasing convection and provides a

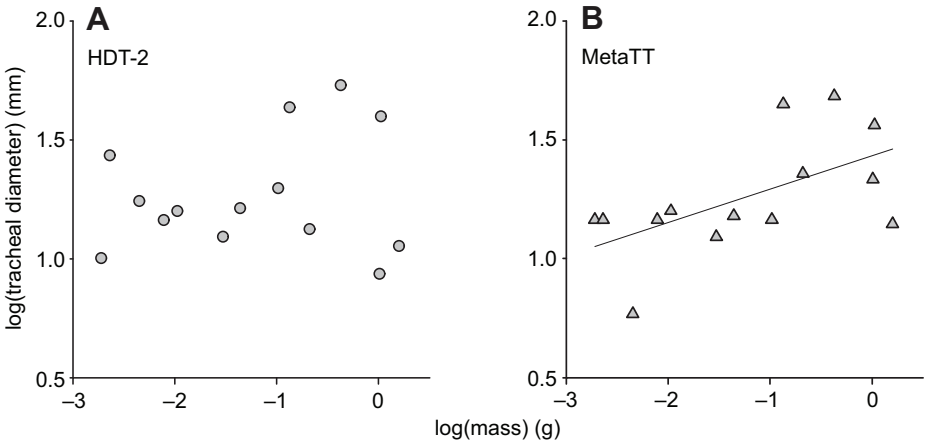

Fig. 8. Regressions of tracheal diameter *versus* body mass for two tracheae. (A) Representative trachea from the head, which does not scale with body mass. (B) Thoracic tracheae scale isometrically with body mass [log tracheal diameter=(0.25log mass) + 1.44]. Metathoracic transverse tracheae shown. See Fig. 7 for tracheae locations.

mechanism for the finding that animals become hypoxic as they near the end of an instar. Overall, our results suggest that the abdominal pumping/tracheal compression behavior of larger caterpillars is a size-based, compensatory mechanism for gas exchange in times of decreased oxygen availability.

Our results are in contrast to those from tracheae in adult beetles (Kaiser et al., 2007) and air sacs in growing grasshoppers (Greenlee et al., 2009), which scale hypermetrically with mass. A study using tracheal diameters from larval, wandering *Drosophila melanogaster* did not scale with body mass (Henry and Harrison, 2004), although the range of masses was too small to infer scaling relationships. Interestingly, in developing grasshoppers, tracheal scaling of two dorsal transverse tracheae exhibited isometric growth in diameter, but hypermetric growth in length (Harrison et al., 2005). Perhaps tracheae in the head of *M. sexta* larvae increase in length rather than diameter. Alternatively, proliferation of tracheae smaller than what we could visualize with synchrotron X-ray imaging could help insects to match oxygen delivery needs as body size increases. These data indicate that measures of tracheal diameter alone are not sufficient to determine how tracheae grow during juvenile development and suggest that measures of length changes of tracheae in *M. sexta*, which routinely grow by 50% of their initial body length within an instar (K.J.G., personal observation), would be useful. Together, these results highlight the need for more studies of tracheal system scaling and suggest that patterns of tracheal investment in larval, holometabolous insects may differ from that of adults and of hemimetabolous insects.

Although caterpillars may not experience hypoxia routinely in nature, it is possible that tracheae are occluded during molting, resulting in localized hypoxia. During experimental hypoxia exposure, body contractions were coordinated to drive gas exchange, as evidenced by the high synchrony between CO_2 emission peaks and both external body movements and tracheal compressions (Fig. 1). The close similarity between abdominal pumping behavior and that observed during molting (Chapman, 1998) provides circumstantial evidence that oxygen limitation may be a signal for ecdysis in insects. Ecdysis, the act of removing the old cuticle, involves three types of abdominal movement: pumping, rotation and peristalsis. During the 20 min ecdysial phase in crickets, abdominal contractions help to extricate the insect from its old cuticle (Carlson, 1977). In pharate moths, eclosion hormone stimulates a central pattern generator that results in abdominal rotations and peristaltic bursts (Truman and Sokolove, 1972). In larval *M. sexta*, two pairs of motor neurons on each abdominal ganglion are responsible for activating the compression muscles of each segment that contract during ecdysis (Novicki and Weeks, 2000). It is unknown whether these ecdysis-triggering neurons also respond to hypoxia. In grasshoppers, some abdominal neurons are sensitive to hypoxia and increase firing rate in response to low oxygen (Bustami et al., 2002). Finally, in *Drosophila*, oxygen-sensitive neuronal cells were discovered that are required for larval ecdysis and adult eclosion (Morton et al., 2008). Together, these studies provide evidence for the hypothesis that hypoxia response observed in the older caterpillars mimics their molting behavior.

ACKNOWLEDGEMENTS

We would like to thank Jordan Boe, Art Woods, Andy Toth, Elizabeth Stanford, Elizabeth Nyberg and Kathryn Jackson for assistance with data collection, Ashley Zondervan for data analysis, and two anonymous reviewers for their helpful comments.

AUTHOR CONTRIBUTIONS

K.J.G., S.D.K. and W.-K.L. concieved this study and designed the experiments. Experiments were executed by K.J.G., S.D.K., W.-K.L. and H.B.E. Data analysis and interpretation was performed by H.B.E., K.J.G., S.D.K., P.P. and J.J.S. Drafting and revision of the article was conducted by K.J.G., S.D.K., W.-K.L. and J.J.S.

COMPETING INTERESTS

No competing interests declared.

FUNDING

This work was supported by the National Science Foundation [EPS-0447679, IOS-0953297 to K.J.G. and EFRI-0938047 to J.J.S.], the National Institutes of Health (NIH) National Center for Research Resources [2P20RR0l5566 to K.J.G.] and the Institute for Critical Technology and Applied Science [118130 to J.J.S.]. The contents of this study are solely the responsibility of the authors and do not necessarily reflect the views of the NIH. Use of the Advanced Photon Source at Argonne National Laboratory was supported by the US Department of Energy, Office of Science, Office of Basic Energy Sciences [DE-AC02-06CH11357]. Deposited in PMC for release after 12 months.

REFERENCES

Benjamini, Y. and Hochberg, Y. (1995). Controlling the false discovery rate: a practical and powerful approach to multiple testing. *J. R. Stat. Soc. B* **57**, 289-300.
Benjamini, Y. and Yekutieli, D. (2001). The control of false discovery rate under dependency. *Ann. Stat.* **29**, 1165-1188.
Blossman-Myer, B. L. and Burggren, W. W. (2010). Metabolic allometry during development and metamorphosis of the silkworm *Bombyx mori*: analyses, patterns, and mechanisms. *Physiol. Biochem. Zool.* **83**, 215-231.
Bustami, H. P., Harrison, J. F. and Hustert, R. (2002). Evidence for oxygen and carbon dioxide receptors in insect CNS influencing ventilation. *Comp. Biochem. Physiol.* **133A**, 595-604.
Calder, W. A., III (1981). Scaling of physiological processes in homeothermic animals. *Annu. Rev. Physiol.* **43**, 301-322.

Callier, V. and Nijhout, H. F. (2011). Control of body size by oxygen supply reveals size-dependent and size-independent mechanisms of molting and metamorphosis. *Proc. Natl. Acad. Sci. USA* **108**, 14664-14669.
Carlson, J. R. (1977). The imaginal ecdysis of the cricket (*Teleogryllus oceanicus*). *J. Comp. Physiol. A* **115**, 299-317.
Chapman, R. F. (1998). *The Insects: Structure and Function*. Cambridge: Cambridge University Press.
Eaton, J. L. (1988). *Lepidopteran Anatomy*. New York, NY: Wiley-Interscience.
Glazier, D. S. (2005). Beyond the '3/4-power law': variation in the intra- and interspecific scaling of metabolic rate in animals. *Biol. Rev. Camb. Philos. Soc.* **80**, 611-662.
Greenlee, K. J. and Harrison, J. F. (2004a). Development of respiratory function in the American locust *Schistocerca americana*. I. Across-instar effects. *J. Exp. Biol.* **207**, 497-508.
Greenlee, K. J. and Harrison, J. F. (2004b). Development of respiratory function in the American locust *Schistocerca americana*. II. Within-instar effects. *J. Exp. Biol.* **207**, 509-517.
Greenlee, K. J. and Harrison, J. F. (2005). Respiratory changes throughout ontogeny in the tobacco hornworm caterpillar, *Manduca sexta*. *J. Exp. Biol.* **208**, 1385-1392.
Greenlee, K. J., Nebeker, C. and Harrison, J. F. (2007). Body size-independent safety margins for gas exchange across grasshopper species. *J. Exp. Biol.* **210**, 1288-1296.
Greenlee, K. J., Henry, J. R., Kirkton, S. D., Westneat, M. W., Fezzaa, K., Lee, W. K. and Harrison, J. F. (2009). Synchrotron imaging of the grasshopper tracheal system: morphological and physiological components of tracheal hypermetry. *Am. J. Physiol.* **297**, R1343-R1350.
Harrison, J. F. (2009). Respiratory system. In *Encyclopedia of Insects*, 2nd edn (ed. V. H. Resh and R. Carde), pp. 889-895. San Diego, CA: Academic Press.
Harrison, J. F., Lafreniere, J. J. and Greenlee, K. J. (2005). Ontogeny of tracheal dimensions and gas exchange capacities in the grasshopper, *Schistocerca americana*. *Comp. Biochem. Physiol.* **141A**, 372-380.
Harrison, J., Frazier, M. R., Henry, J. R., Kaiser, A., Klok, C. J. and Rascón, B. (2006). Responses of terrestrial insects to hypoxia or hyperoxia. *Respir. Physiol. Neurobiol.* **154**, 4-17.
Henry, J. R. and Harrison, J. F. (2004). Plastic and evolved responses of larval tracheae and mass to varying atmospheric oxygen content in *Drosophila melanogaster*. *J. Exp. Biol.* **207**, 3559-3567.
Kaiser, A., Klok, C. J., Socha, J. J., Lee, W.-K., Quinlan, M. C. and Harrison, J. F. (2007). Increase in tracheal investment with beetle size supports hypothesis of oxygen limitation on insect gigantism. *Proc. Natl. Acad. Sci. USA* **104**, 13198-13203.
Kestler, P. (1985). Respiration and respiratory water loss. In *Environmental Physiology and Biochemistry of Insects* (ed. K. H. Hoffmann), pp. 137-183. Berlin: Springer-Verlag.
Morton, D. B., Stewart, J. A., Langlais, K. K., Clemens-Grisham, R. A. and Vermehren, A. (2008). Synaptic transmission in neurons that express the *Drosophila* atypical soluble guanylyl cyclases, Gyc-89Da and Gyc-89Db, is necessary for the successful completion of larval and adult ecdysis. *J. Exp. Biol.* **211**, 1645-1656.
Narum, S. R. (2006). Beyond Bonferroni: less conservative analyses for conservation genetics. *Conserv. Genet.* **7**, 783-787.
Novicki, A. and Weeks, J. C. (2000). Developmental attenuation of *Manduca* pre-ecdysis behavior involves neural changes upstream of motoneurons and relay interneurons. *J. Comp. Physiol. A* **186**, 69-79.
Ojeda-Avila, T., Woods, H. A. and Raguso, R. A. (2003). Effects of dietary variation on growth, composition, and maturation of Manduca sexta (Sphingidae: Lepidoptera). *J. Insect Physiol.* **49**, 293-306.
Peters, R. H. (1983). *The Ecological Implications of Body Size*. Cambridge: Cambridge University Press.
Sears, K. E., Kerkhoff, A. J., Messerman, A. and Itagaki, H. (2012). Ontogenetic scaling of metabolism, growth, and assimilation: testing metabolic scaling theory with *Manduca sexta* larvae. *Physiol. Biochem. Zool.* **85**, 159-173.
Socha, J. J., Westneat, M. W., Harrison, J. F., Waters, J. S. and Lee, W.-K. (2007). Real-time phase-contrast X-ray imaging: a new technique for the study of animal form and function. *BMC Biol.* **5**, 6.
Truman, J. W. and Sokolove, P. G. (1972). Silk moth eclosion: hormonal triggering of a centrally programmed pattern of behavior. *Science* **175**, 1491-1493.
Wasserthal, L. T. (1996). Interaction of circulation and tracheal ventilation in holometabolous insects. *Adv. Insect Physiol.* **26**, 297-351.

Movie 1. This movie shows the synchronization between the external body movements and the tracheal compressions during hypoxia in a fifth instar caterpillar. The top panel shows the light video we recorded, and the bottom panel shows the X-ray video taken at the same time.

Movie 2. This X-ray video shows tracheal movements in normoxia and hypoxia in a fourth instar caterpillar.